

Determination of the capture cross sections of electrons in undoped hydrogenated amorphous silicon from the photoconductivity of and space-charge relaxation in  $n^+ - i - n^+$  structures; the role of light exposure and annealing

This article has been downloaded from IOPscience. Please scroll down to see the full text article.

2001 J. Phys.: Condens. Matter 13 5663

(<http://iopscience.iop.org/0953-8984/13/24/311>)

View [the table of contents for this issue](#), or go to the [journal homepage](#) for more

Download details:

IP Address: 171.66.16.226

The article was downloaded on 16/05/2010 at 13:33

Please note that [terms and conditions apply](#).

# Determination of the capture cross sections of electrons in undoped hydrogenated amorphous silicon from the photoconductivity of and space-charge relaxation in $n^+ - i - n^+$ structures; the role of light exposure and annealing

M Meaudre and R Meaudre

Département de Physique des Matériaux (UMR 5586 CNRS), Université Lyon I,  
43 Boulevard du 11 Novembre 1918, 69622 Villeurbanne Cédex, France

E-mail: rmeaudre@dpm.univ-lyon1.fr

Received 22 February 2001

## Abstract

Electron capture cross sections,  $\sigma_c$ , in standard hydrogenated amorphous silicon deposited at 150 °C are determined from photoconductivity (PC) and space-charge-relaxation (SCR) measurements. A good correlation is observed between the values obtained by the two techniques. The validity of the methods used is tested by varying  $\sigma_c$  over a large range by light-soaking. It is shown that the capture cross sections depend strongly on the density of states at the Fermi level  $N(E_F)$ ; in fact,  $\sigma_c$  increases by nearly two orders of magnitude when  $N(E_F)$  increases by only a factor of five. The PC and SCR studies both account for this large increase.

## 1. Introduction

There is considerable scatter of the values of the cross sections  $\sigma_c$  for capture of electrons by the mid-gap density of states in undoped hydrogenated amorphous silicon (a-Si:H) in the literature. Values of  $\sigma_c$  ranging from  $10^{-18}$  cm<sup>2</sup> to  $10^{-15}$  cm<sup>2</sup> have been obtained depending on the samples and experiments [1–11]. The first aim of this paper is to compare the values of  $\sigma_c$  derived for  $n^+ - i - n^+$  a-Si:H samples by two completely independent techniques, one appealing to photoconductivity and the other to space-charge relaxation. It will be shown that two mathematical approaches to the same physical model can be used to describe space-charge relaxation. Following on from this, the second aim of this work is to decide which of the mathematical approaches is better on the basis of a comparison of the  $\sigma_c$ -values derived from the two experimental techniques. Finally, in order to check against merely fortuitous coincidence of  $\sigma_c$ -values, these values will be determined by the two techniques and compared while a treatment is given to the samples as a result of which  $\sigma_c$  is varied by about two orders of magnitude.

## 2. Samples and experimental procedure

Standard a-Si:H films are obtained by rf (13.56 MHz) glow discharge decomposition of pure silane in a multiplasma monochamber reactor described elsewhere [12].  $n^+i-n^+$  sandwich structures are deposited with  $\text{SnO}_2$  on the bottom electrode and 2 mm diameter Al dots as the top electrode; the thicknesses of the  $n^+$  and  $i$  layers are 50 nm and in the range 4–7  $\mu\text{m}$  respectively. As  $\text{SnO}_2$  reduction can occur at 250 °C contaminating the  $i$  layer, the substrate temperature is kept at 150 °C. The experiments were all performed in a vacuum of  $10^{-6}$  Torr: the dark conductivity  $\sigma_d$  and the activation energy  $E_a$  of  $\sigma_d$  are derived from conductivity–temperature characteristics (DC), the densities of states at the Fermi level  $N(E_F)$  are extracted from space-charge-limited-current (SCLC)  $I$ – $V$  characteristics at 306 K, and the electron capture cross sections,  $\sigma_c$ , are deduced from two independent techniques: measurements of the photoconductivity (PC) at  $\lambda = 750$  nm and the space-charge relaxation (SCR), both at 306 K. Experimental details related to all of these measurements are given in previous papers [3, 13, 14]. The absorption coefficient  $\alpha$  is determined from photothermal deflection spectroscopy and transmission measurements performed on a  $\sim 1$   $\mu\text{m}$   $i$  layer deposited under the same conditions. First, samples are annealed at 150 °C for three hours (state A); then they are exposed to 40  $\text{mW cm}^{-2}$  water-filtered white light produced by a 1 kW halogen lamp for 400 min at 30 °C (at certain time intervals the illumination is interrupted to make the series of electrical measurements). After this light-soaking (state B), they are subjected to successive thermal dark annealings,  $a_1, a_2, a_3, \dots, a_8$ ; the temperature and duration of each of these are specified later on. The DC, SCLC, PC, and SCR are measured for samples in state A, at different stages of light-soaking, in state B, and at different stages of annealing.

## 3. The models used to derive the cross sections $\sigma_c$ for capture of electrons by the mid-gap density of states

### 3.1. Determination of $\sigma_c$ in $n^+i-n^+$ structures from dc photoconductivity (PC) measurements

3.1.1. *Calculation of the volume carrier generation rate  $G$  in the  $i$  layer.* A Corning-glass– $\text{SnO}_2$   $n^+i-n^+$  Al structure is illuminated through the Corning glass. The number of electron–hole pairs excited per second at the distance  $x$  from the  $n^+i$  interface is

$$G(x) = \alpha N_{ph} \exp(-\alpha x) + \alpha R N_{ph} \exp(-2\alpha L) \exp(\alpha x). \quad (1)$$

$N_{ph}$  is the incident photon flux corrected for reflection and absorption in the  $\text{SnO}_2$  and  $n^+$  layer,  $\alpha$  is the coefficient of absorption in the  $i$  layer of thickness  $L$ , and  $R$  is the reflectivity at the back a-Si:H/Al interface.

In order to be able to derive the photoconductivity of the  $i$  layer easily from the photocurrent when using a sandwich structure, one must manage to keep the excess-carrier density and the rate  $G$  nearly constant as functions of  $x$ . We chose to measure the photoconductivity at the wavelength  $\lambda = 750$  nm for which  $\alpha = 300 \text{ cm}^{-1}$  and  $\alpha L = 0.15$ . Under these conditions, equation (1) with  $R = 0.8$  leads to  $G(0) = 1.59\alpha N_{ph}$  and  $G(L) = 1.55\alpha N_{ph}$ , so we took  $G(x) = G = 1.55\alpha N_{ph}$  as a good approximation.

3.1.2. *The expression for the photoconductivity.* In undoped a-Si:H the photoconductivity is dominated by electrons and is given by

$$\sigma_{ph}(x) = e\mu_n \Delta n(x) = e\mu_n G(x)\tau(x) \quad (2)$$

which for the experimental situation described above reduces to

$$\sigma_{ph}(x) = \sigma_{ph} = e\mu_n G\tau \quad (3)$$

where  $\Delta n = n - n_0$  is the excess-electron density in the conduction band,  $n_0$  the equilibrium density of electrons,  $\mu_n$  and  $\tau$  their mobility and lifetime, respectively.

With  $N(E)$  the density of states in the gap of a-Si:H, according to Taylor and Simmons [15] one has

$$\tau = \left[ \sigma_c v \int_{E_F}^{E_{tn}} N(E) dE \right]^{-1} \quad (4)$$

where  $v$  is the thermal velocity of electrons,  $\sigma_c$  the capture cross section of the gap states for electrons (assumed to be independent of energy),  $E_F$  is the Fermi level. The quasi-Fermi level  $E_{tn}$  for trapped electrons is given by

$$E_{tn} = E_F + kT \ln \left[ \frac{\sigma_p p + \sigma_c n}{\sigma_c n_0} \right] \quad (5)$$

where  $\sigma_p$  and  $p$  are the capture cross section for holes and the free-hole density respectively.

In a-Si:H one has  $\sigma_c n \gg \sigma_p p$  [8], so equation (5) reduces to

$$E_{tn} = E_F + kT \ln \frac{n}{n_0} \quad (6)$$

which shows that  $E_{tn}$  coincides with the quasi-Fermi level for free electrons  $E_{Fn}$ , and then

$$\tau = \left[ \sigma_c v \int_{E_F}^{E_{Fn}} N(E) dE \right]^{-1}. \quad (7)$$

Let us assume that the shape of the density of states above the Fermi level is given by

$$N(E) = N(E_F) \exp[(E - E_F)/E_0]. \quad (8)$$

The parameter  $E_0$  characterizes the shape of  $N(E)$  [16].

From equations (7) and (8), one immediately gets

$$\tau^{-1} = \sigma_c v N(E_F) E_0 [\exp(\Delta E_F/E_0) - 1] \quad (9)$$

with  $\Delta E_F = E_{Fn} - E_F$ .

From equation (6) one obtains

$$\frac{n}{n_0} = 1 + \frac{\Delta n}{n_0} = \exp(\Delta E_F/kT)$$

and

$$\Delta n = G\tau = \frac{G}{\sigma_c v N(E_F) E_0} \left( 1 + \frac{\Delta n}{n_0} \right)^{-kT/E_0}. \quad (10)$$

Our experimental situation corresponds to  $\Delta n/n_0 \gg 1$ ; thus

$$(\Delta n)^{(E_0+kT)/E_0} = \frac{G}{\sigma_c v N(E_F) E_0 (n_0)^{-kT/E_0}}. \quad (11)$$

Two important consequences follow from equation (11). First

$$\sigma_{ph} = e\mu_n \Delta n \propto G^\gamma \quad (12)$$

with

$$\gamma = \frac{E_0}{E_0 + kT}. \quad (13)$$

Second, the capture cross section  $\sigma_c$  can now be deduced from photoconductivity and conductivity measurements. Indeed with  $\sigma_d = n_0 e \mu_n$  the dark conductivity, the calculation of  $\sigma_c$  is straightforward:

$$\sigma_c = G \left( \frac{\sigma_d}{e\mu_n} \right)^{(1/\gamma-1)} \left/ \left[ v N(E_F) E_0 \left( \frac{\sigma_{ph}}{e\mu_n} \right)^{1/\gamma} \right] \right. \quad (14)$$

Hence provided that  $\mu_n$  and  $v$  are known and the value of  $N(E_F)$  is obtained from SCLC measurements, the value of  $\sigma_c$  can be calculated.

### 3.2. Determination of $\sigma_c$ from space-charge-relaxation (SCR) measurements

3.2.1. *The model of Solomon [17].* Let us just recall the principle of the measurement. A space charge is first electrically created in the i layer of an  $n^+ - i - n^+$  structure by a high voltage  $V_H$ ; it is due to injected electrons that have been trapped on gap states above the Fermi level in the intrinsic layer. At time  $t = 0$ , the bias  $V_H$  is dropped to a very low value; the potential barrier due to the space charge decreases the conductivity of the device. The trapped electrons will be thermally re-excited in the conduction band, decreasing the barrier over time, and the current imposed by the low voltage will increase to its equilibrium value. Let us now describe the relaxation of the space charge. At time  $t$  the negative density of charge  $\rho(t)$  is supposed to be uniformly distributed along the i layer and the integration of Poisson's equation gives the value of the potential produced by the trapped charges between the two extremities  $x = 0$  and  $x = L$  of the i layer. The height of the potential barrier at  $x = L/2$  is easily derived and the current is given by

$$\frac{i_0}{i(t)} = \exp \left[ -\frac{1}{8} \frac{e\rho(t)L^2}{\varepsilon\varepsilon_0kT} \right] \quad (15)$$

where  $-e$  is the electron charge and  $i_0$  is the current at equilibrium, without a space charge.  $\rho(t)$  is now calculated by considering the kinetics of release of trapped electrons into the conduction band.

$N_T(E, t)$  is the density of electrons trapped on gap states of energy  $E$ , at a given time  $t$ ; these electrons will be excited into the conduction band at a rate  $\nu(E)$ . The electrons are then swept out of the intrinsic region by the electric field due to space charge, so retrapping by gap states can be neglected and one has

$$\frac{\partial N_T(E, t)}{\partial t} = -\nu(E)N_T(E, t) \quad (16)$$

where

$$\nu(E) = \nu_0 \exp[-(E_C - E)/kT] \quad (17)$$

and  $\nu_0$  is the 'attempt-to-escape' frequency,  $E_C$  the conduction band mobility edge.

The solution of equation (16) is

$$N_T(E, t) = N_T(E, t = 0) \exp[-\nu(E)t]. \quad (18)$$

$\rho(t)$  is given by

$$\rho(t) = -e \int_{E_V}^{E_C} [N_T(E, t) - N_{T0}(E)] dE \quad (19)$$

where  $N_{T0}(E)$  is the normal density of electrons in gap states at equilibrium.

Solomon [17] now gives

$$\rho(t) = -e \int_{E_V}^{E_C} [N_T(E, t = 0) - N_{T0}(E)] \exp[-\nu(E)t] dE \quad (20)$$

which, providing that  $\nu(E_F)t > 3$ , leads to

$$\rho(t) = -eN(E_F)kT/\nu(E_F)t. \quad (21)$$

From equations (15) and (21), the relaxation of the current is now obtained:

$$1/\ln[i_0/i(t)] = \frac{8\varepsilon\varepsilon_0\nu(E_F)t}{e^2N(E_F)L^2}. \quad (22)$$

The values of  $\sigma_c$  are then derived as follows. From the experimental value of  $\nu(E_F)$  and equation (17), the value of  $\nu_0$  is derived using  $E_C - E_F = E_a$ ,  $E_a$  being the activation energy of the dark conductivity. Now from detailed balance consideration one immediately gets

$$\nu_0 = \sigma_c \nu N(E_C) kT \quad (23)$$

and  $\sigma_c$  is calculated with the usual values of  $\nu$  and  $N(E_C)$  [18].

**3.2.2. The model of Solomon revisited [19].** For the sake of simplicity Solomon [17] chose to derive  $\rho(t)$  from equation (20); however, we observe that equations (18) and (19) impose in fact

$$\rho(t) = -e \int_{E_V}^{E_C} [N_T(E, t = 0) \exp(-\nu(E)t) - N_{T0}(E)] dE. \quad (24)$$

Therefore in a recent paper [19], we re-examined this model. Relaxation at long times was calculated taking retrapping of electrons into account, with the result that equation (16) has been replaced by

$$\frac{\partial N_T(E, t)}{\partial t} = -\nu(E)N_T(E, t) + \sigma_c \nu n(t)[N(E) - N_T(E, t)] \quad (25)$$

where  $n(t)$  is the electron density in the conduction band of the  $i$  layer.

Equation (25) was then integrated leading to

$$\rho(t) = -eN(E_F)kT \frac{[\exp(-\nu(E_F)t)]}{\nu(E_F)t}$$

and

$$i_0/i(t) = \exp \left[ \frac{e^2 L^2 N(E_F)}{8\epsilon\epsilon_0 \nu(E_F)t} e^{-\nu(E_F)t} \right]. \quad (26)$$

The values of  $\nu(E_F)$  are then derived from plots of  $\ln[i_0/i(t)]$  on a logarithmic scale versus time and  $\sigma_c$  is calculated as in the previous paragraph.

## 4. Results and discussion

### 4.1. Annealed and light-soaked states

The aim of this work is to determine the capture cross sections in standard a-Si:H using the above-described techniques, to compare them, and so to test the validity of the methods used. To check against merely fortuitous coincidence of values obtained, we varied the electron capture cross sections over a large range by light-soaking and annealing, and we first characterized the sample state using the parameters  $\sigma_d$ ,  $E_a$ , and  $N(E_F)$ . Initially (state A), the measured  $N(E_F)$  is  $7 \times 10^{15} \text{ cm}^{-3} \text{ eV}^{-1}$ , independent of the applied voltage polarity. Samples were then irradiated through the  $\text{SnO}_2$ ;  $N(E_F)$  increases with time of irradiation faster on the  $\text{SnO}_2$  side than on the Al side, but the difference between the values obtained at different stages of irradiation does not exceed a factor of two. After a  $40 \text{ mW cm}^{-2}$  irradiation for 400 min, we obtained  $N(E_F) = 3.5 \times 10^{16} \text{ cm}^{-3} \text{ eV}^{-1}$  (state B); the irradiation was stopped and the samples were annealed; finally  $N(E_F)$  was  $9 \times 10^{15} \text{ cm}^{-3} \text{ eV}^{-1}$  (state C). We note that the values of  $N(E_F)$  determined from state B to state C are similar whatever the electron injection is from the  $\text{SnO}_2$  or the Al electrode. In the following we only consider the results concerning samples having a nearly homogeneous distribution of defects—that is to say, the samples in state A, in state B, and in the states obtained after annealings  $a_1, a_2, \dots, a_8$  (i.e. from state B to state C). The parameters  $\sigma_d$ ,  $E_a$ ,  $N(E_F)$  determined for each sample state are reported in table 1. As expected from the standard Staebler–Wronski effect,  $\sigma_d$  decreases and  $E_a$  increases when  $N(E_F)$  increases.

**Table 1.** Characteristics of samples measured in state A, state B, and after successive thermal dark annealings,  $a_1, a_2, \dots, a_8$ , from state B to state C. The annealing temperature and time are indicated for each of them.

	State A	State B	$a_1$	$a_2$	$a_3$
	180 min	400 min	60 min	60 min	30 min
	150 °C	40 mW cm <sup>-2</sup>	65 °C	95 °C	125 °C
$\sigma_d(306 \text{ K}) \text{ (S cm}^{-1}\text{)}$	$1.9 \times 10^{-9}$	$6.3 \times 10^{-11}$	$6.1 \times 10^{-11}$	$7.5 \times 10^{-11}$	$1.6 \times 10^{-10}$
$E_a \text{ (eV)}$	0.7	0.81	0.78	0.77	0.76
$N(E_F) \text{ (cm}^{-3} \text{ eV}^{-1}\text{)}$	$7 \times 10^{15}$	$3.5 \times 10^{16}$	$3 \times 10^{16}$	$3 \times 10^{16}$	$3 \times 10^{16}$
	$a_4$	$a_5$	$a_6$	$a_7$	$a_8$ , state C
	60 min	180 min	180 min	180 min	180 min
	125 °C	150 °C	150 °C	150 °C	150 °C
$\sigma_d(306 \text{ K}) \text{ (S cm}^{-1}\text{)}$	$2.5 \times 10^{-10}$	$1.3 \times 10^{-9}$	$2 \times 10^{-9}$	$2.9 \times 10^{-9}$	$3.6 \times 10^{-9}$
$E_a \text{ (eV)}$	0.74	0.7	0.68	0.68	0.68
$N(E_F) \text{ (cm}^{-3} \text{ eV}^{-1}\text{)}$	$2.7 \times 10^{16}$	$1.6 \times 10^{16}$	$1.2 \times 10^{16}$	$1.1 \times 10^{16}$	$9 \times 10^{15}$

#### 4.2. $\sigma_c$ -values deduced from photoconductivity measurements

Typical photoconductivity variations measured at 750 nm for a carrier generation rate between  $10^{14}$  and  $10^{18} \text{ cm}^{-3} \text{ s}^{-1}$  are given in figure 1 for different states of the sample. We observe a power-law behaviour:  $\sigma_{ph} \propto G^\gamma$  with  $0.68 < \gamma < 0.8$  for a photon flux varying by four orders of magnitude. Such variations are expected if the shape of the density of states above

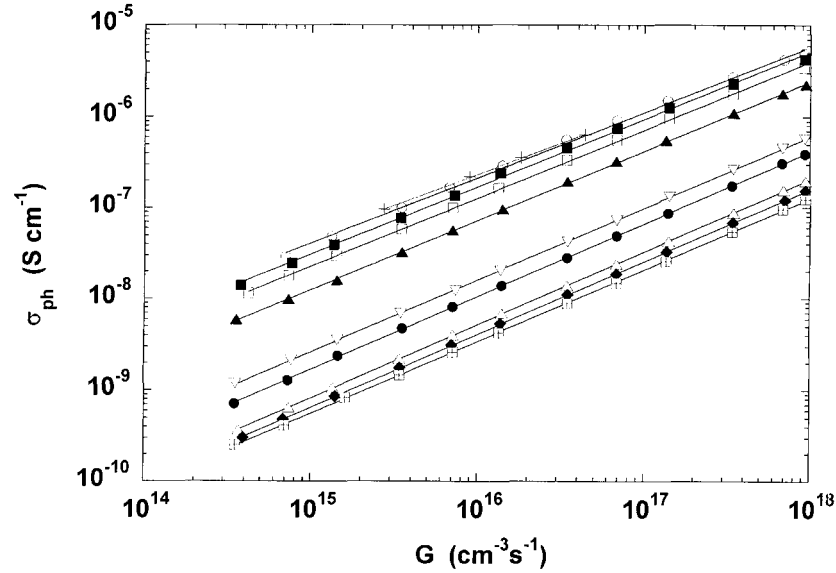


**Figure 1.** Photoconductivity measured at  $\lambda = 750 \text{ nm}$  against volume generation rate  $G$  for different sample states: (+) initial state (state A), ( $\oplus$ ) after  $40 \text{ mW cm}^{-2}$  white-light irradiation (state B), ( $\blacklozenge$ ) after  $a_1$ , ( $\Delta$ ) after  $a_2$ , ( $\bullet$ ) after  $a_3$ , ( $\nabla$ ) after  $a_4$ , ( $\blacktriangle$ ) after  $a_5$ , ( $\square$ ) after  $a_6$ , ( $\blacksquare$ ) after  $a_7$ , ( $\circ$ ) after  $a_8$  (state C).  $a_1, a_2, \dots, a_8$  are successive thermal annealings. The temperature and time of each of them are given in tables 1, 2, 3.

the Fermi level is given by

$$N(E) = N(E_F) \exp \frac{E - E_F}{E_0}$$

where  $E_0$  is a characteristic parameter of the distribution; in this case  $\gamma = E_0/(E_0 + kT)$  (equations (12) and (13)).  $\gamma$  and  $E_0$  can be deduced from figure 1. Taking into account all of the parameters given in table 2 and assuming  $\mu_n = 10 \text{ cm}^2 \text{ V}^{-1} \text{ s}^{-1}$  and  $v = 1.1 \times 10^7 \text{ cm s}^{-1}$ , we have calculated  $\sigma_c$  from equation (14) and figure 1 (table 2).

**Table 2.**  $\sigma_c$ -values obtained from PC measurements reported in figure 1 and equation (14).  $\gamma$ ,  $E_0$ ,  $\sigma_d$ ,  $N(E_F)$ : parameters used for the calculation.

	State A 180 min 150 °C	State B 400 min 40 mW cm <sup>-2</sup>	a <sub>1</sub> 60 min 65 °C	a <sub>2</sub> 60 min 95 °C	a <sub>3</sub> 30 min 125 °C
$\gamma$	0.69	0.785	0.80	0.8	0.8
$E_0$ (meV)	55	95	97	104	104
$\sigma_d(306 \text{ K})$ (S cm <sup>-1</sup> )	$1.9 \times 10^{-9}$	$6.3 \times 10^{-11}$	$6.1 \times 10^{-11}$	$7.5 \times 10^{-11}$	$1.6 \times 10^{-10}$
$N(E_F)$ (cm <sup>-3</sup> eV <sup>-1</sup> )	$7 \times 10^{15}$	$3.5 \times 10^{16}$	$3.1 \times 10^{16}$	$3 \times 10^{16}$	$2.7 \times 10^{16}$
$\sigma_c[\text{PC}]$ (cm <sup>2</sup> )	$1.7 \times 10^{-18}$	$3.2 \times 10^{-17}$	$3 \times 10^{-17}$	$8.8 \times 10^{-18}$	$1.2 \times 10^{-17}$
	a <sub>4</sub> 60 min 125 °C	a <sub>5</sub> 180 min 150 °C	a <sub>6</sub> 180 min 150 °C	a <sub>7</sub> 180 min 150 °C	a <sub>8</sub> , state C 180 min 150 °C
$\gamma$	0.79	0.76	0.75	0.74	0.72
$E_0$ (meV)	96	82	78	75	68
$\sigma_d(306 \text{ K})$ (S cm <sup>-1</sup> )	$2.5 \times 10^{-10}$	$1.3 \times 10^{-9}$	$2 \times 10^{-9}$	$2.9 \times 10^{-9}$	$3.6 \times 10^{-9}$
$N(E_F)$ (cm <sup>-3</sup> eV <sup>-1</sup> )	$2 \times 10^{16}$	$1.6 \times 10^{16}$	$1 \times 10^{16}$	$1 \times 10^{16}$	$9 \times 10^{15}$
$\sigma_c[\text{PC}]$ (cm <sup>2</sup> )	$9.7 \times 10^{-18}$	$3 \times 10^{-18}$	$2.9 \times 10^{-18}$	$2.6 \times 10^{-18}$	$2.3 \times 10^{-18}$

#### 4.3. $\sigma_c$ -values deduced from space-charge-relaxation measurements

The relaxation of the conductivity of our films after different electrical injections of electrons as well as the experimental details have been reported in previous papers [3, 19]. In a first approach, we considered Solomon's model [17] and plotted  $1/\ln[i_0/i(t)]$  versus time (figure 2). The evolution given by equation (22) is verified by the experiment for long times.  $N(E_F)$  being known, the slope of the straight line (figure 2) and equation (22) lead to the experimental  $v(E_F)$ . We then derive the  $\sigma_c$ -values from equations (17) and (23) using  $E_C - E_F = E_a$ ,  $v = 1.1 \times 10^7 \text{ cm s}^{-1}$ , and  $N(E_C) = 2 \times 10^{21} \text{ cm}^{-3}$ . The  $\sigma_c$ -values obtained are reported in table 3.

The second approach [19] more rigorously predicts a different variation of space-charge relaxation with time; it seems interesting to re-examine our experimental data on the basis of these new theoretical calculations. As expected from equation (26), a plot of  $\ln(i_0/i(t))$  on a logarithmic scale versus time leads to a straight line for long times (figure 3). The values of  $\sigma_c$  are derived from fitting the long-tail relaxation using equation (26).

#### 4.4. Discussion

A comparison of the  $\sigma_c$ -values derived from PC and SCR measurements is given in figures 4 and 5. A good correlation is observed between the values obtained with the two techniques. However, figure 4 shows that the values derived from the SCR with Solomon's model are much



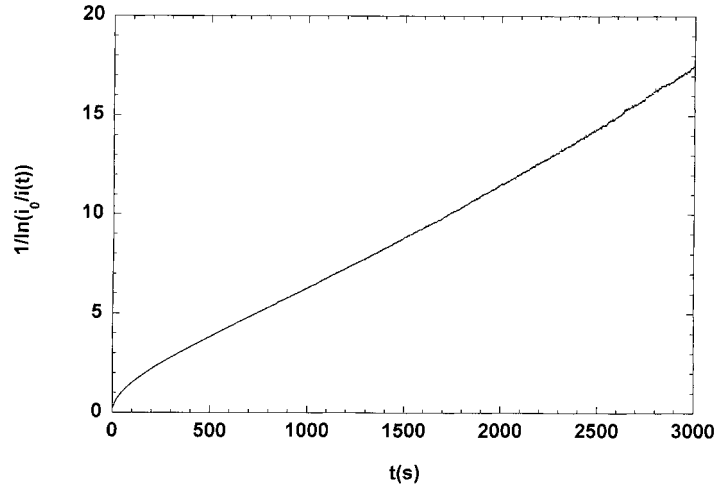


**Figure 2.** An example of relaxation of the current  $i(t)$  after electrical injection of electrons into the intrinsic layer. This plot can be analysed in terms of equation (22). Applied voltage  $V = 20$  mV. Sample thickness =  $5 \mu\text{m}$ .

**Table 3.**  $\sigma_c$ -values obtained from SCR measurements.  $\sigma_c$ [SCR1]: values calculated with equation (22) (Solomon's model);  $\sigma_c$ [SCR2]: values calculated with equation (26) (Solomon's model revisited).  $E_a$  and  $N(E_F)$ : parameters used for the calculation.

	State A 180 min 150 °C	State B 400 min 40 mW cm <sup>-2</sup>	a <sub>1</sub> 60 min 65 °C	a <sub>2</sub> 60 min 95 °C	a <sub>3</sub> 30 min 125 °C
$\sigma_d$ (S cm <sup>-1</sup> )	$2.5 \times 10^{-9}$	$6.3 \times 10^{-11}$	$6.1 \times 10^{-11}$	$7.5 \times 10^{-11}$	$1.6 \times 10^{-10}$
$E_a$ (eV)	0.7	0.81	0.78	0.77	0.76
$N(E_F)$ (cm <sup>-3</sup> eV <sup>-1</sup> )	$7 \times 10^{15}$	$3.5 \times 10^{16}$	$3.1 \times 10^{16}$	$3 \times 10^{16}$	$2.7 \times 10^{16}$
$\sigma_c$ [SCR1] (cm <sup>2</sup> )	$9.4 \times 10^{-17}$	$3.4 \times 10^{-14}$	$1.3 \times 10^{-14}$	$5.5 \times 10^{-15}$	$4.9 \times 10^{-15}$
$\sigma_c$ [SCR2] (cm <sup>2</sup> )	$7.7 \times 10^{-19}$	$5.2 \times 10^{-17}$	$4.3 \times 10^{-17}$	$1 \times 10^{-17}$	$9.5 \times 10^{-18}$
	a <sub>4</sub> 60 min 125 °C	a <sub>5</sub> 180 min 150 °C	a <sub>6</sub> 180 min 150 °C	a <sub>7</sub> 180 min 150 °C	a <sub>8</sub> , state C 180 min 150 °C
$\sigma_d$ (S cm <sup>-1</sup> )	$2.5 \times 10^{-10}$	$1.3 \times 10^{-9}$	$2 \times 10^{-9}$	$2.9 \times 10^{-9}$	$3.6 \times 10^{-9}$
$E_a$ (eV)	0.74	0.7	0.68	0.68	0.68
$N(E_F)$ (cm <sup>-3</sup> eV <sup>-1</sup> )	$2 \times 10^{16}$	$1.6 \times 10^{16}$	$1 \times 10^{16}$	$1 \times 10^{16}$	$9 \times 10^{15}$
$\sigma_c$ [SCR1] (cm <sup>2</sup> )	$1.6 \times 10^{-15}$	$4.7 \times 10^{-16}$	$2.8 \times 10^{-16}$	$7.3 \times 10^{-17}$	$7 \times 10^{-17}$
$\sigma_c$ [SCR2] (cm <sup>2</sup> )	$4.3 \times 10^{-18}$	$1.7 \times 10^{-18}$	$1.2 \times 10^{-18}$	$6 \times 10^{-19}$	$6 \times 10^{-19}$

higher than those derived from the PC measurements, while our version of the SCR model leads to a good agreement between  $\sigma_c$ -values derived from the PC and SCR (figures 5 and 6). It is remarkable that techniques so different lead to practically identical results. However, the fact that the two techniques give a good agreement between  $\sigma_c$ -values is not so surprising. Indeed, according to equations (11) and (12),  $\sigma_{ph}$  is dominated by those states with the lowest  $\sigma_c$ , and according to equations (17), (22), (23), and (26), it is clear that long-tail relaxation is also dominated by those states with the lowest  $\sigma_c$ -values.

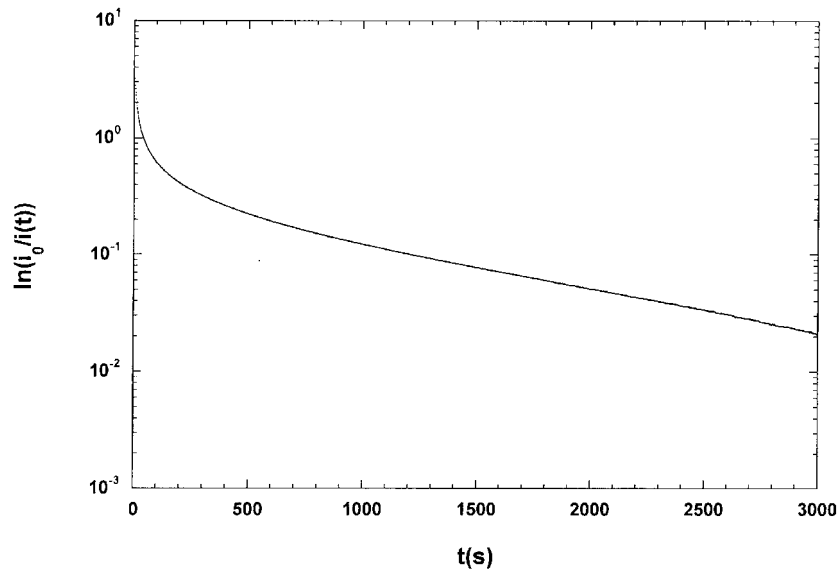


**Figure 3.** The same relaxation of the current  $i(t)$  as in figure 2. The long-tail variation given by equation (26) is verified.

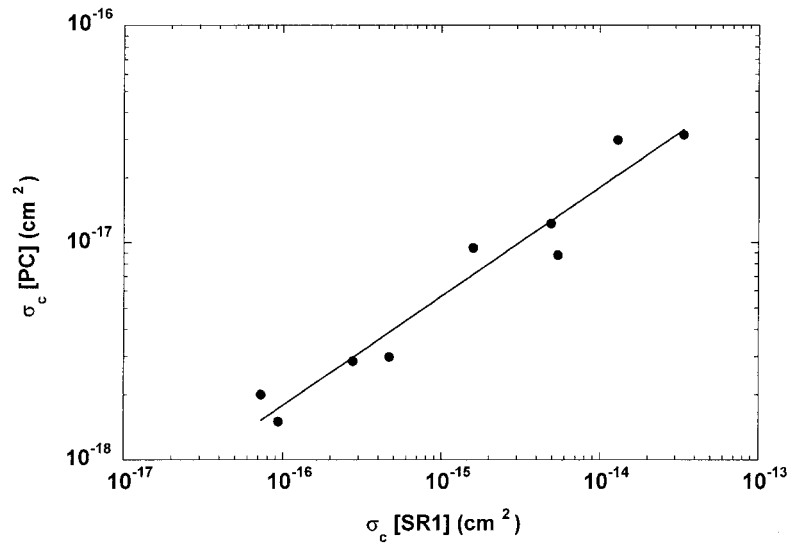


**Figure 4.** Comparison of the values of the capture cross sections derived from the photocurrent ( $\sigma_c$ [PC]) and from the space-charge relaxation ( $\sigma_c$ [SCR1]) calculated from equation (22). The line is a guide for the eyes.

The  $\sigma_c$ -values measured in our standard films (state A),  $(1-5) \times 10^{-18} \text{ cm}^2$ , are lower than the values generally estimated for a-Si:H, but it must be recalled that the distribution of capture cross sections given in the literature spans three or more decades,  $10^{-18}-10^{-15} \text{ cm}^2$  [1-11]. Our measured  $\sigma_c$ -values, though low, are not in contradiction with results obtained earlier by other authors.

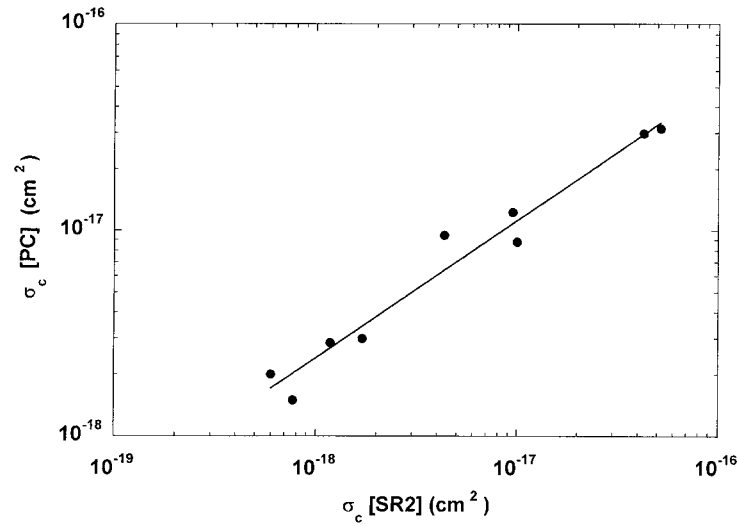


**Figure 5.** Comparison of the values of the capture cross sections derived from the photocurrent ( $\sigma_c$ [PC]) and from the space-charge relaxation ( $\sigma_c$ [SCR2]) calculated from equation (26). The line is a guide for the eyes.

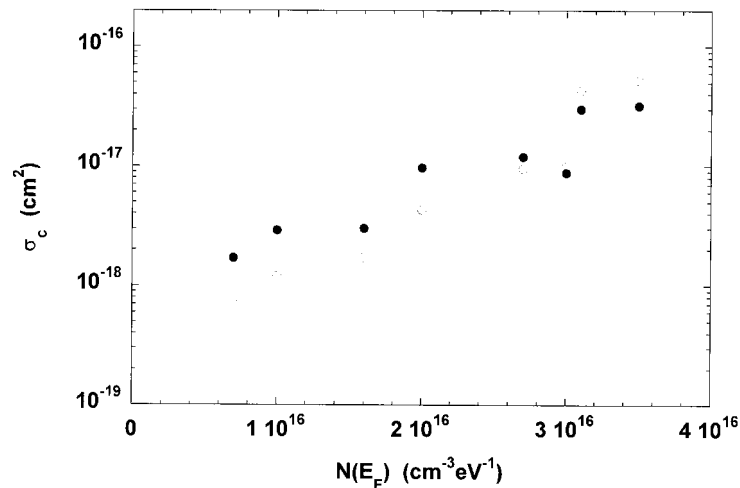


**Figure 6.** Variations of capture cross sections  $\sigma_c$  as a function of the density of states at the Fermi level  $N(E_F)$ . ●:  $\sigma_c$ [PC]; ○:  $\sigma_c$ [SCR2].

The aim of this paper was not to study light-soaking effects in a-Si:H, since a considerable amount of work has already been carried out in this field. However, we note in passing that the results in figure 1 fully confirm that a moderate increase of the defect density by a factor of 3–4 can decrease the photoconductivity  $\sigma_{ph}$  by two orders of magnitude. Clearly, other parameters and especially an increase of  $\sigma_c$  must be invoked to give an account of the observation; in fact,  $\sigma_c$  increases by a factor of about 50 when  $N(E_F)$  increases by a factor of 5 (figure 6). Kounavis and Mytilineou observed an increase of  $\sigma_c/\mu$  by a factor of about 10 when the defect density increased by a factor of about 2 [10]. This all seems to confirm the accuracy of the  $\sigma_c$ -values determined for our films.

## 5. Conclusions

Faced with two mathematical approaches to space-charge relaxation (SCR) in  $n^+i-n^+$  a-Si:H structures, we chose to compare the electron capture cross sections  $\sigma_c$  of mid-gap states deduced from the SCR techniques and from a completely independent one, namely the photoconductivity (PC) technique. A good correlation between  $\sigma_c$ -values has been observed using the SCR and PC; however, better agreement was obtained when a rigorous treatment of the SCR taking retrapping of electrons into account was used.

For a-Si:H deposited and annealed at 150 °C, having  $N(E_F) = (7-9) \times 10^{15} \text{ cm}^{-3} \text{ eV}^{-1}$ , we have obtained  $\sigma_c = (1-5) \times 10^{-18} \text{ cm}^2$  from PC and SCR measurements. For light-soaked a-Si:H, having  $N(E_F) = (3.5-4) \times 10^{16} \text{ cm}^{-3} \text{ eV}^{-1}$ , again PC and SCR studies give quite similar values:  $\sigma_c = (3-6) \times 10^{-17} \text{ cm}^2$ . It must be underlined that the two techniques both account for this large increase. This result is in agreement with the observation of Kounavis and Mytilineou [10]: from investigation of the modulated photocurrent they found that  $\sigma_c$  increased by one order of magnitude upon light-soaking while the defect density increased only by a factor of two. For all of these reasons, we are inclined to be confident of the procedure used to determine electron capture cross sections in our films.

## Acknowledgments

This work was partially supported by the Centre National de la Recherche Scientifique and Agence pour le Développement et la Maîtrise de l'Énergie ECODEV programme.

## References

- [1] Stutzmann M, Jackson W B and Tsai C C 1985 *Phys. Rev. B* **32** 23
- [2] Cech V, Schauer F and Stuchlik J 1998 *J. Non-Cryst. Solids* **227-230** 185
- [3] Meaudre R, Meaudre M, Butté R and Vignoli S 1999 *Phil. Mag. Lett.* **79** 763
- [4] Street R A, Biegelsen D K and Weisfield R L 1984 *Phys. Rev. B* **30** 5861
- [5] Bube R H, Benatar L E and Bube K P 1996 *J. Appl. Phys.* **79** 1926
- [6] Pandya R and Schiff E A 1985 *J. Non-Cryst. Solids* **77-78** 623
- [7] Kounavis P, Mataras D and Rapakoulias D 1996 *J. Appl. Phys.* **80** 2305
- [8] Arene E and Baixeras J 1984 *Phys. Rev. B* **30** 2016
- [9] Hack M and Shur M 1985 *J. Appl. Phys.* **58** 997
- [10] Kounavis P and Mytilineou E 1995 *Solid State Phenom.* **44-46** 715
- [11] Hack M and Shur M 1985 *J. Appl. Phys.* **58** 997
- [12] Roca i Cabarrocas P, Chevrier J P, Huc J, Lloret A, Parey J Y and Schmitt J P M 1991 *J. Vac. Sci. Technol. A* **9** 2331
- [13] Meaudre M, Jensen P and Meaudre R 1991 *Phil. Mag. B* **63** 815
- [14] Meaudre M, Meaudre R, Butté R, Vignoli S, Longeaud C, Kleider J P and Roca i Cabarrocas P 1999 *J. Appl. Phys.* **86** 946
- [15] Taylor G W and Simmons J G 1972 *J. Non-Cryst. Solids* **8-10** 940
- [16] Rose A 1963 *Concepts in Photoconductivity and Allied Problems* (New York: Interscience)
- [17] Solomon I 1995 *J. Non-Cryst. Solids* **190** 107
- [18] Street R A 1991 *Hydrogenated Amorphous Silicon* (Cambridge: Cambridge University Press)
- [19] Meaudre R and Meaudre M 2001 *J. Phys.: Condens. Matter* submitted